Modeling and Simulation of an AUV-Towfish System

Lea G. Miller
Dept. Ocean & Mechanical Engineering
Florida Atlantic University
Dania Beach, FL USA

Karl D. von Ellenrieder
Dept. Ocean & Mechanical Engineering
Florida Atlantic University
Dania Beach, FL USA
ellenrie@fau.edu

***Abstract*— Simulations of an autonomous underwater vehicle, tow cable, and magnetometer towfish are performed using a combined Matlab-Orcaflex interface to provide a better understanding of how changes in towing speed (0.5 – 2m/s), cable length (5 – 15m), vehicle trajectory (circle and vertical zig zag maneuvers), and current speed (0.25 – 1.25m/s) affect towfish trajectory. The AUV-towfish system consists of a Bluefin autonomous underwater vehicle (AUV) and a Seaspy towed magnetometer. The simulations reveal that a 5m tow cable provides the best maneuverability of the towfish in comparison to longer cables. The towfish traveled a greater distance in a given period of time and more closely followed the waypoints of the AUV in not only the x and y directions, but in the vertical direction as well. The longer tow cables gave the towfish too much freedom to stray off course during maneuvering of the AUV. Tow speeds between 60% and 80% thrust showed provide better towfish pitch angles than slower tow speeds. While 80% thrust showed the best towfish pitch results, this fast speed may not be desirable when attempting to collect magnetic field data. Surface current speeds between 0.25m/s and 1.25m/s altered the courses of the AUV and towfish during circular maneuvering. As the surface current speed increased up to 1.25m/s the AUV-towfish system could no longer maintain course.**

Keywords— Dynamic Simulation, AUV, towfish

I. Introduction

This work is part of a larger effort to characterize how oceanographic features, such as currents, tides, internal waves, strong shear, and vertical mixing can act to redistribute the temperature, salinity and density within the water column and thereby affect the magnetic and electric fields within and about a region of the ocean. To accomplish this, an electromagnetic observatory and a field observation and analysis program are being developed to study the impact of oceanographic processes on electro-magnetic fields in the coastal waters off of Southeast Florida, USA. Surface buoys and bottom-mounted moorings will be used to capture cross-shelf and along-shelf variability in the water column. Each surface buoy will be equipped with a microCAT chain, a downward-looking ADCP, a directional wave staff, an EM sensor (in air), and on one of the buoys, a met station. Each of the bottom-mounted stations will be equipped with a microCAT chain, an ADCP, a pressure sensor and an EM sensor. The bottom-mounted station closest to shore will capture surf-zone dynamics while the other stations will provide real time information about the variability of currents, waves, temperature, and salinity at shallow to intermediate depths. Each of the stations will simultaneously record local electric and magnetic signals.

Additionally, a mobile AUV platform will be utilized to survey small regions of interest within the observatory as guided by real-time data from the fixed sensors. The AUV will be equipped with upward and downward looking ADCPs, a CTD and will tow a magnetometer. The benefits of using a towfish mounted magnetometer are that the arrangement will enable a larger separation distance between noise generating sources on the AUV and the magnetic sensor than would be possible with an AUV-mounted magnetometer [1], [2], [6] and that the towfish can provide a stable measurement platform for the measurements [12], [19]. Further, it is anticipated that the use of the AUV in combination with the fixed and moored oceanographic sensors will present an opportunity to help understand the link between measured local and large scale variability within the water column [9]. Since internal waves travel along thermoclines and the effects of internal wave propagation on background electromagnetic fields are of special interest, the possibility of using the AUV-towfish system to perform measurements at or near the thermocline [8] is another compelling reason for its planned implementation. It has been shown that the fluctuations caused by internal waves are on the order of 0.1 to 1.0 nT [4]; the Earth's magnetic field is 45000 nT and so both platform stability and platform generated noise are special concerns.

In order to better understand the dynamical interaction between the AUV and towfish before the offshore experiments are conducted, computer modeling and simulation have been performed to characterize the effects of towing speed, cable length, current and course changes on the stability and trajectory of the system. The objectives are to determine the effects changes in cable length (5 – 15 m), towing speed (0.5 – 2 m/s), vehicle trajectory (circle and vertical zig zag maneuvers), and current (0.25 – 1.25 m/s) will have on the different outputs, such as towfish trajectory and orientation. Waypoints generating circle and zig zag patterns represent typical maneuvers used for tracking internal waves within the thermocline and are representative of motions the system will experience during field testing.

II. Approach

A. The AUV-Towfish System

The AUV-towfish system will consist of a Bluefin autonomous underwater vehicle (AUV) and a Seaspy towed

This work was sponsored by the Office of Naval Research under grant N000141010939 (Program Manager: Dr. Stephen Potashnik).

magnetometer. The AUV (Fig. 1) can be broken down into three major sections: tail, parallel mid-body and nose section with lengths of 1.19 m, 0.61 m, and 1.07 m, respectively [5], which gives a total length of 2.87 m. The diameter of the vehicle is 0.533 m. The AUV has a total mass of approximately 250 kg and is typically operated at speeds of between 0.5 to 2.0 m/s [5], [14], [15]. The vehicle is outfitted with a Conductivity, Temperature and Depth (CTD) sensor, as well as both upward looking and downward looking 300-1200 kHz Acoustic Doppler Current Profilers (ADCPs) for measuring current speeds in the water column.

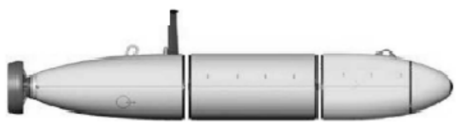

Fig. 1 Bluefin AUV [5].

The Seaspy magnetometer towfish (Fig. 2) uses an Overhauser sensor that measures the magnitude of the magnetic field. The magnetometer has a sensitivity of 0.01 nT and a resolution of 0.001 nT [11].

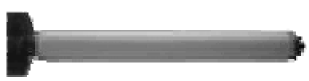

Fig. 2 Seaspy magnetometer towfish [12].

The towfish has a length of 1.24 m and a diameter of 0.127 m. Its weight in air is 16 kg and weight in water is 2 kg [11]. The towfish has three flat plate fins, separated by 120 degrees from each other. Cord length and span of the fins are 0.09 m and 0.3 m, respectively. The longitudinal center of gravity was measured to be 0.63 m from the aft end, and the longitudinal center of buoyancy was calculated to be 0.61 m from the aft end.

The manufacturer of the Seaspy magnetometer towfish provides two tow cable options: positively buoyant or negatively buoyant. Since the cable will be fully submerged for this experiment, the positively buoyant cable was selected. The cable was modeled as an umbilical with a specified outer diameter and weight in air as shown in TABLE I. The bending diameter is the minimum diameter the cable is capable of bending, and the breaking strength is the maximum force allowable before the cable is ruptured.

B. Simulation Models

The AUV and towfish models were developed in Matlab Version 7.11. The dynamics and kinematics of the AUV and towfish are governed by motions in the x, y, and z axes. The body and inertial axes in relation to the AUV and towfish body are shown in Fig. 3 and Fig. 4, respectively. The origin of the body-fixed coordinates is located at the center of buoyancy of each body.

Velocities are represented in each direction as shown by u (surge), v (sway), and w (heave). Euler's angles φ, θ, and ψ represent roll, pitch, and yaw, and rotation rates are *p*, *q*, and *r*. The positive direction follows the right hand rule for each axis; for example, positive roll is to starboard, positive yaw is to starboard, and positive pitch is nose up. The state vector can therefore be written as [3], [16], [17]:

$$\vec{X} = \begin{bmatrix} X_I \\ \Theta_I \\ V \\ \Omega \end{bmatrix} \quad (1)$$

where

$$\vec{X} = \begin{bmatrix} X_I \\ \Theta_I \\ V \\ \Omega \end{bmatrix}, \overrightarrow{\Theta_I} = \begin{bmatrix} \varphi \\ \theta \\ \psi \end{bmatrix}, \vec{V} = \begin{bmatrix} u \\ v \\ w \end{bmatrix}, \overrightarrow{\Omega} = \begin{bmatrix} p \\ q \\ r \end{bmatrix}. \quad (2)$$

TABLE I TOW CABLE PROPERTIES

Property	Value
Outer diameter	0.019 m
Bending diameter	0.25 m
Weight in air	0.125 kg/m
Weight in water	-0.020 kg/m
Breaking strength	2500 kg

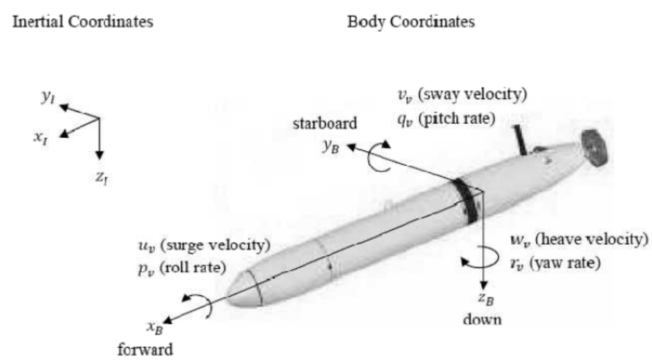

Fig. 3 Bluefin AUV Inertial and Body Coordinates.

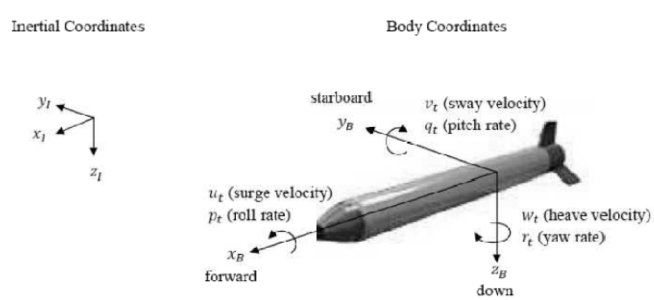

Fig. 4 Seaspy Magnetometer Inertial and Body Coordinates.

The transformation matrix R_{IB} is used to change from body-fixed coordinates to inertial coordinates [10]:

$$R_{IB} = \begin{bmatrix} c\psi\, c\theta & -s\psi\, c\varphi + c\psi\, s\theta\, s\varphi & s\psi\, s\,\varphi + c\,\psi\;c\,\varphi\, s\,\theta \\ s\,\psi\, c\,\theta & c\,\psi\;c\,\varphi + s\,\varphi\, s\,\theta\, s\,\psi & -c\,\psi\;s\,\varphi + s\,\theta\, s\,\psi\, c\,\varphi \\ -s\,\theta & c\,\theta\, s\,\varphi & c\,\theta\, c\,\varphi \end{bmatrix} \tag{3}$$

The translational kinematic equation is defined using the rotation matrix:

$$\dot{\vec{X_I}} = R_{IB}\vec{V}. \tag{4}$$

Rotation rates are related to the time rate of change of Euler's equations using the rotational kinematic equation [3], [16], [17]:

$$\begin{bmatrix} \dot{\varphi} \\ \dot{\theta} \\ \dot{\psi} \end{bmatrix} = \begin{bmatrix} 1 & \sin\varphi\tan\theta & \cos\varphi\tan\theta \\ 0 & \cos\varphi & -\sin\varphi \\ 0 & \sin\varphi/\cos\theta & \cos\varphi/\cos\theta \end{bmatrix} \begin{bmatrix} p \\ q \\ r \end{bmatrix}. \tag{5}$$

Kirchoff's equations of motion for a rigid body in an ideal fluid [10], [16], [17] are defined as:

$$\begin{bmatrix} \vec{M} & D^T \\ D & \vec{J} \end{bmatrix} \begin{bmatrix} \dot{\vec{V}} \\ \dot{\vec{\Omega}} \end{bmatrix} = \begin{bmatrix} \left(\vec{MV} + D^T\vec{\Omega}\right) \times \vec{\Omega} + \vec{F}_{ext} \\ \left(\vec{J\Omega} + D\vec{V}\right) \times \vec{\Omega} + \left(\vec{MV} + D^T\vec{\Omega}\right) \times \vec{V} + \vec{M}_{ext} \end{bmatrix}, \tag{6}$$

where the sum of the external forces and moments acting on the AUV and towfish are:

$$\vec{F}_{ext} = \begin{bmatrix} F_x \\ F_y \\ F_z \end{bmatrix} = \vec{F}_{weight} + \vec{F}_{buoyancy} + \vec{F}_{body} + \vec{F}_{tail} + \vec{F}_{cable}, \tag{7}$$

$$\vec{M}_{ext} = \begin{bmatrix} M_x \\ M_y \\ M_z \end{bmatrix} = \vec{M}_{CG} + \vec{M}_{body} + \vec{M}_{tail} + \vec{M}_{damping} + \vec{M}_{cable}. \tag{8}$$

A more descriptive breakdown of the equations of motion and maneuvering coefficients used for this research can be found in reference [13].

C. Model Validation

1) AUV Model Validation

A series of simulations of the Bluefin AUV were conducted and compared to data from field tests and simulations of a similar Bluefin AUV [14], [15]. Field tests showed that providing 58% thrust gave a resulting surge of approximately 1.5 m/s [14]. A simple AUV simulation with a constant forward thrust and no deflection of the rudder or sternplane was generated to validate the speed of the vehicle. The vehicle model reached a steady state surge speed of approximately 1.75 m/s with a thrust level of 58%. A speed of 1.5 m/s was obtained when the thrust was reduced to 50%, and therefore a percent thrust of 50% was used for AUV model validation.

Differing propeller models is a possible cause for the different speed results. Similarities between the model used in reference [14] and the model developed as a part of this research include a maximum propeller speed of 500 RPM, and a thrust deduction factor of 0.1. Differences between the two propellers were thrust and torque coefficient. The model used in this report estimated these coefficients using reference [7] for a ducted thruster.

The model was set up to run a simulation similar to the field test described in [14]. Fig. 5 shows the change in AUV heading from rudder deflections for this simulation. The time delay was approximately 5 seconds for each execution. An approximate 6.5 degree offset occurred between the heading response and actual rudder deflection. This is 1.5 degrees greater offset than the 5 degree offset that was reported during field testing [14].

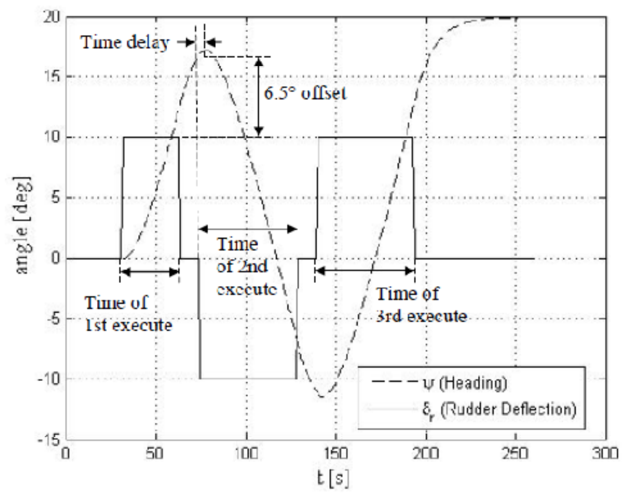

Fig. 5 AUV Heading change from rudder deflection.

The sternplane deflection shown in Fig. 6 was tested using a 200 second long simulation. The vehicle was set to follow a straight course while the sternplane was deflected to cause the vehicle to ascend and descend. For the first 30 seconds, the sternplane was set to 0 degrees. The first execution deflected the sternplane 5 degrees in the positive z-direction (recall z is positive downward), which caused the vehicle to ascend after an initial time delay of approximately 5 seconds. At time equal to 60 seconds, the sternplane deflection was changed to -5 degrees. The time delay for the vehicle to change direction in the 2nd and 3rd cases where the sternplane is immediately deflected in the opposite direction was approximately 20 seconds. Reference [14] reported having no detection of a sternplane offset in the data or during experiments.

2) Towfish Model Validation

The towfish model was verified using a similarly shaped towed vehicle described in [18]. The comparative towed vehicle has a length of 2.59 m and a mass of 113.5 kg. The Seaspy towfish model was set to run at a depth of 30 m and move forward at 3 m/s using the AUV model as the driving force for the free end of the cable. The length of the cable in this model was a 100 m long umbilical, which is equal to the cable length between the towed vehicle and the depressor. Fig. 7 shows the surge and heave motions of the towfish. Fig. 7 a) shows the surge velocity to rise up to 3 m/s after approximately 10 seconds. For the first 10 seconds of Fig. 7 b), the towfish experiences a rising heave motion that is caused by a slightly negative pitch due to the 0.0118 m separation between the center of gravity and center of buoyancy. The heave velocity rises to 0.5 m/s as the towfish begins to move and then drops to nearly 0 m/s as the towfish reaches a steady state surge velocity of 3 m/s.

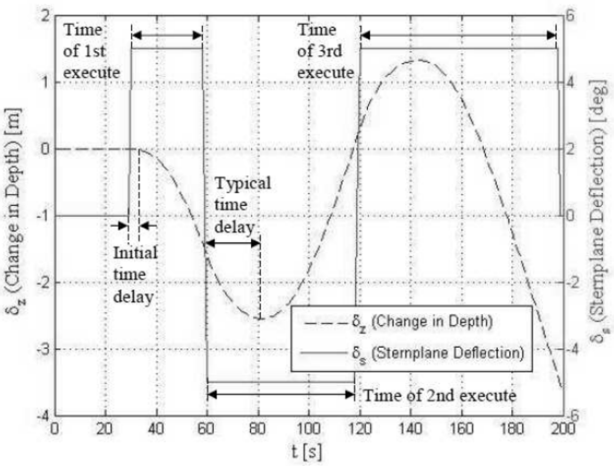

Fig. 6 AUV depth change from sternplane deflection: The vehicle heave position (--) is measured with the scale on the left and sternplane deflection (—) is measured with the scale on the right.

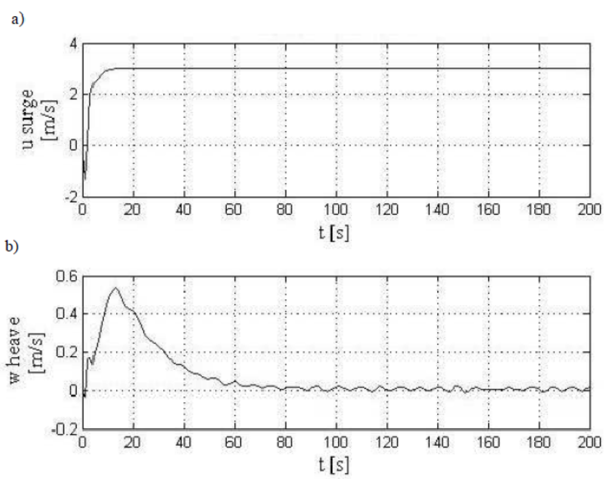

Fig. 7 Towfish Velocity Validation: a) surge velocity, b) heave velocity.

Fig. 8 shows the velocities of the towed vehicle. As seen below, the towed vehicle motion does not start from rest, and therefore there is no initial heaving motion of the towed vehicle. The surge velocity continuously makes small oscillations around 3 m/s, while the heave velocity oscillates around 0 m/s with the exception of the time frame 75 – 125 seconds where the heave is between -0.5 m/s and 0.5 m/s. The comparative towed vehicle experiences sea-wave disturbances from the surface vehicle that is towing it, and therefore the towfish model could not duplicate the exact response. However, when looking at the generalized steady state responses of the towed vehicle in motion, the towfish model does have comparable results.

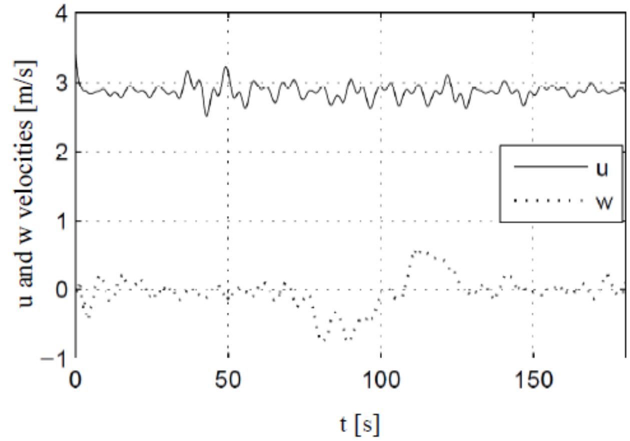

Fig. 8 Towed Vehicle Velocities from [19].

Pitch rates for the towfish and towed vehicle are shown in Fig. 9 and Fig. 10, respectively. The pitch results of the towed vehicle simulation appear to start from rest because of the initial jump in pitch rate up to almost 1 deg/s. The initial pitch rate of the towfish was only 0.25 deg/s. Similar to the conclusions for the heave responses, it is believed the towfish appeared more stable since it did not experience wave disturbances within the simulation that are typically transmitted by a tow vehicle traveling near the free surface.

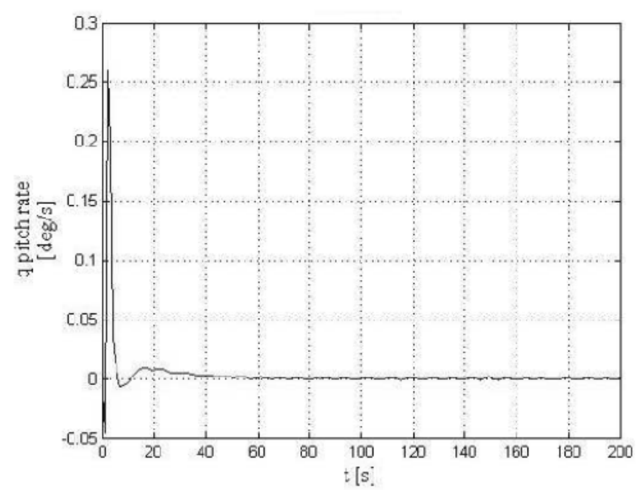

Fig. 9 Towfish Pitch Rate Validation

III. RESULTS

The results are organized into sections based on specific simulation objectives, such as determining cable length. Note that every AUV-towfish simulation was generated at a depth of 30 m, and therefore the z direction trajectories begin at 30 m.

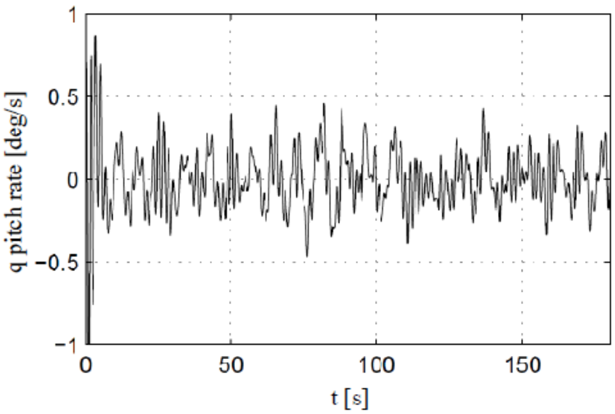

Fig. 10 Towed Vehicle Pitch Rate from [18].

A. Cable Length

To determine an appropriate cable length for the AUV-towfish system, maneuvers and thrust levels were held constant for a set of simulations of varying cable lengths. In addition, different maneuvers were simulated to determine the reactions of the towfish as the cable length was adjusted.

The circle maneuver results showed a significant difference in towfish trajectory in both the y and z directions. As the cable length was increased, the amount of area circled by the towfish decreased. The towfish trajectory followed the AUV trajectory much more closely with the shorter cable lengths, as be seen in Fig. 11 a, b, and c.

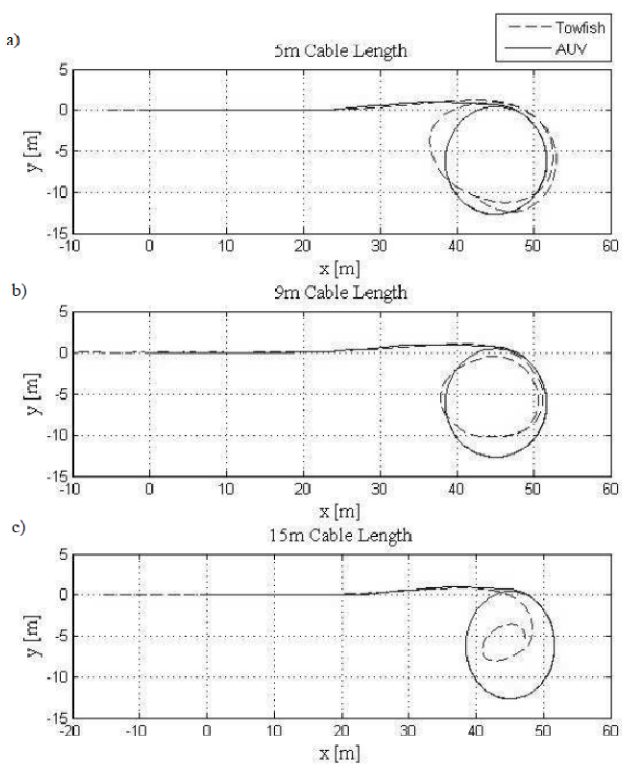

Fig. 11 Trajectories with Various Cable Lengths: a) 5 m cable, b) 9 m cable, c) 15 m cable.

In addition, the depth of the towfish was approximately 30 m during the circle maneuver with a shorter cable length (See Fig. 12 a, b, and c). With a 5 m length cable, the depth stayed between approximately 29 m and 32.5 m. A 9 m cable allowed the towfish to travel between depths of 32 m and 35 m, and a 15 m cable allowed a depth of the towfish to drop into the 39 m to 44 m range. Note that the AUV maintained a constant depth of 30 m for all simulations.

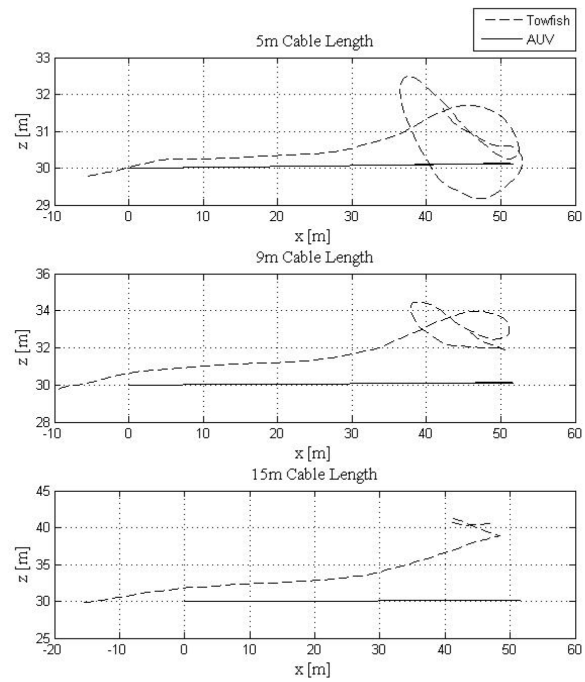

Fig. 12 Towfish Depth Trajectory with Various Cable Lengths: a) 5 m cable, b) 9 m cable, c) 15 m cable.

The vertical zig zag maneuver showed depth coverage similar to the circle maneuver for each cable length. For these simulations, the AUV was programmed to oscillate the sternplane between ± 5 degrees. The towfish responded by covering approximately 5 m of depth in an oscillating pattern for each cable length. However, the longer cable lengths tended to allow the towfish to drop further below the depth of the AUV's course. Depth trajectories for each cable length during this maneuver are shown in Fig. 13. It can be seen that the 5 m cable oscillates between 30 m and 36 m depths, 9 m cable oscillates between 35 m and 40 m depths, and 15 m cable oscillates between 40 m and 46 m depths. These results are quite similar to the depth trajectories shown in Fig. 12.

B. Percent Thrust

Dynamic responses of the towfish and cable were determined for various AUV speeds. For these simulations, the cable length was set constant at 9 m and current speed was 0 m/s. Results for vertical zig zag and circle maneuvering are provided in this section.

Towfish trajectories during vertical zig zag maneuvering showed little change as the thrust was increased. A secondary simulation was done using 15 degree sternplane oscillations, but the results did not show any unexpected towfish behavior that differed from the 5 degree oscillation results.

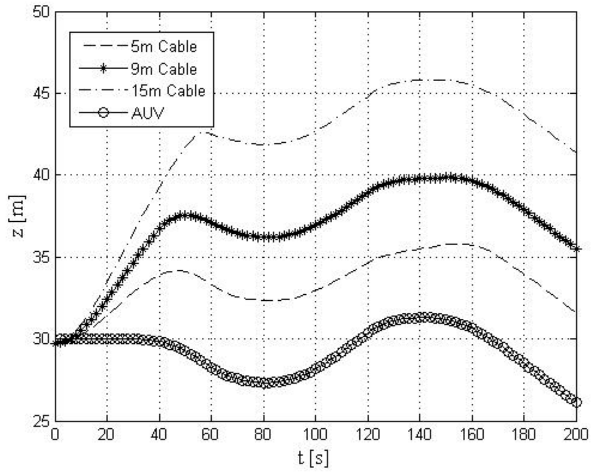

Fig. 13 Vertical Zig Zag Maneuver with Various Cable Lengths.

Trajectory during circle maneuvers with thrusts of 40%, 60%, and 80% are shown in Fig. 14 a, b, and c. With the thrust set at 40% thrust, the towfish travels about 5 m in the y direction and does not quite complete one circle within the 150 second time frame. The distance traveled in y direction increased to almost 10 m with 60% thrust, and the towfish traveled around the circle pattern 1.5 times within the same 150 second time frame. The largest distance covered was achieved with 80% thrust. The towfish traveled approximately 18 m in the y direction and completed the circle trajectory over 1.5 times.

Angular orientation of the towfish was also significantly affected by changes in thrust. When the circle maneuver began at 40% thrust, the roll of the towfish was 30 degrees and then approached approximately 25 degrees for the remainder of the maneuver. Pitch angle increased almost linearly for the first 100 seconds and then reached a steady state at approximately 80 degrees, which is very close to the sensor's 90 degree dead zone.

To determine if the large pitch angle was being caused by the difference in center of gravity and center of buoyancy location, the circle maneuver with 40% and 80% thrust were repeated with 0.01 m less separation between the two points. Results show the pitch angle decreased from 80 degrees to 30 degrees with the 40% thrust, and the pitch angle with 80% thrust decreased from 50 degrees to as low as 10 degrees for most of the simulation.

C. Current

The effects of current conditions were also tested. All of these simulations used a constant thrust of 60% and a linearly decreasing current that dropped 10% in speed every 10m in depth. Circle maneuvering, and zig zag maneuvering were both tested with changing current speeds.

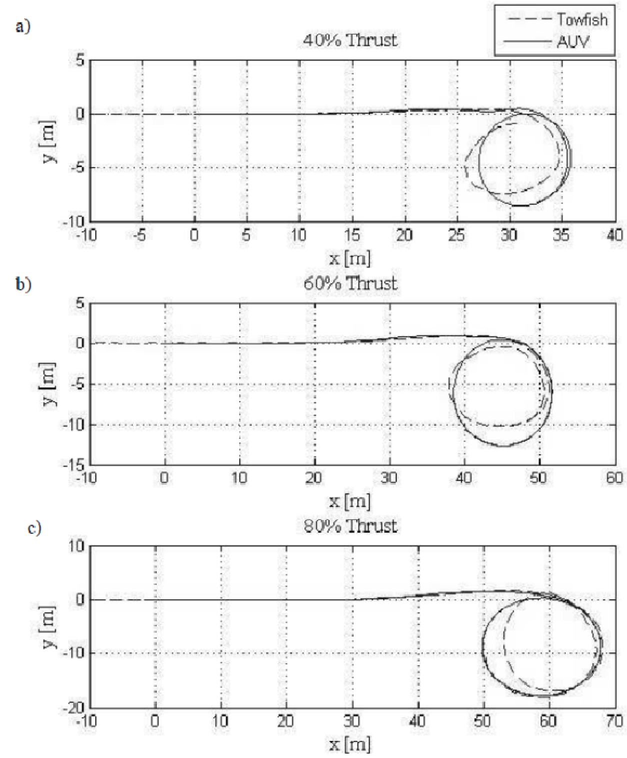

Fig. 14 Trajectories during Circle Manuever with Various Percent Thrusts: a) 40% thrust, b) 60% thrust, c) 80% thrust.

The circle maneuver showed many changes with towfish dynamics as the current was increased. These simulations used a cable length of 9 m. Trajectories of the towfish using surface currents speeds of 0.25 m/s, 0.75 m/s, and 1.25 m/s are shown in Fig. 15, Fig. 16, Fig. 17, respectively.

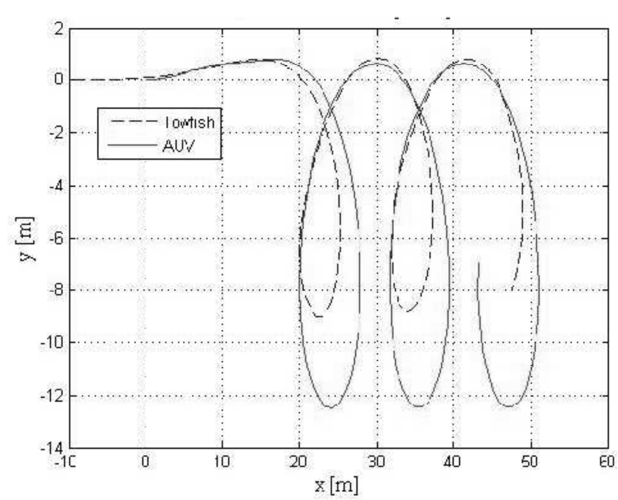

Fig. 15 Circle Maneuver: 0.25 m/s Current.

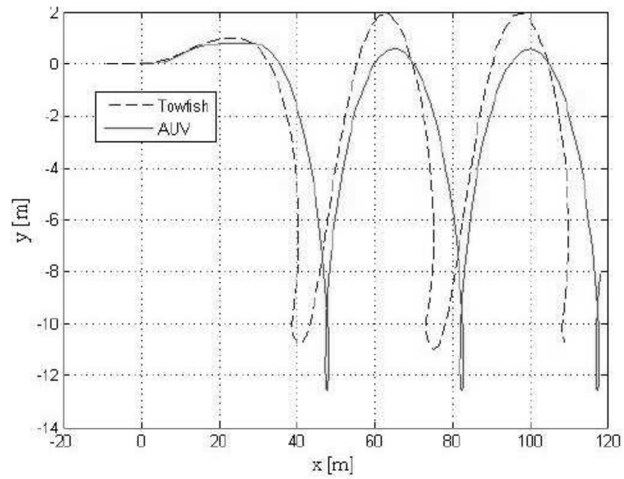

Fig. 16 Circle Maneuver: 0.75m/s Current.

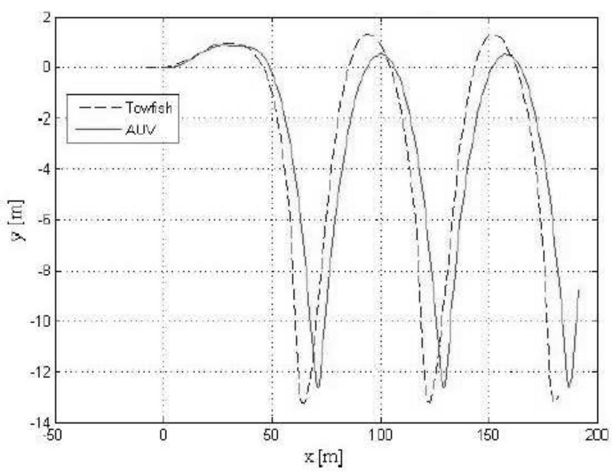

Fig. 17 Circle Maneuver: 1.25m/s Current.

During circular maneuvers with a current, the AUV and towfish trajectory took on a spiral shape in the x and y directions, as expected. At a surface current speed of 0.25 m/s, the AUV and towfish both maintained a circular pattern. As the current speed was increased, the shape became less spiral and more like a zig zag pattern as shown in Fig. 18 with a 1.25 m/s current. However, it did maintain approximately 14 m area coverage in the y direction for all currents. Body velocities did not change significantly.

The set of vertical zig zag maneuvers used a constant thrust of 60%, a 5 degree sternplane oscillation, and a cable length of 9 m. The trajectory of the towfish did not change significantly as the current was increased. There was about a 3 m difference in the depth between 0.25 m/s and 0.75 m/s, but since this depth change did not occur when the current was increased to 1.25 m/s, a direct correlation could not be made between current and change in depth.

D. Tow Cable Tension

Average effective tension for the towfish and AUV during no-current circle maneuvers with a 9 m cable at 60% thrust shown in Fig. 18.

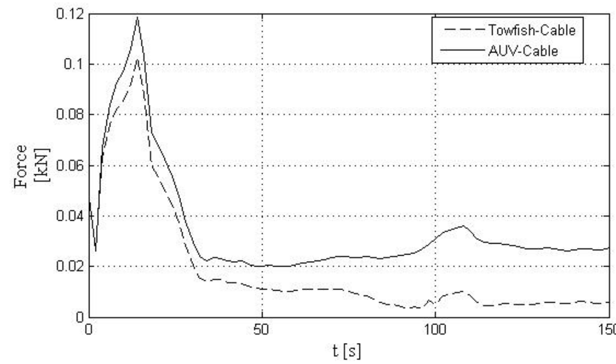

Fig. 18 Effective Tension during Circle Maneuver.

The AUV-towfish system is at rest at the start of the simulation. As the AUV begins to pull the towfish forward in a straight line motion, the tension at the AUV-cable connection and towfish-cable connection rises to 0.12 kN and 0.1 kN, respectively. As soon as the motion of the system begins to turn into a circle maneuver at time equals 15 seconds, the tension begins to drop. There is a slight rise in tension at 110 seconds, which corresponds to a point during the circle maneuver where the AUV and towfish are traveling in opposite directions along the y-axis.

Effective tension at both the AUV-cable and towfish-cable connection points was much lower during vertical zig zag maneuvering, which is shown in Fig. 19 for a 9 m cable and 60% thrust. The greatest tension seen during this maneuver was also at the initial start, where tension reached 0.05 kN at both the AUV-cable connection and towfish-cable connection. Once vertical zig zag maneuvering began, tension at the AUV-cable connection point began to oscillate around approximately 0.029 kN, while tension at the towfish-cable connection point oscillated around 0.001 kN.

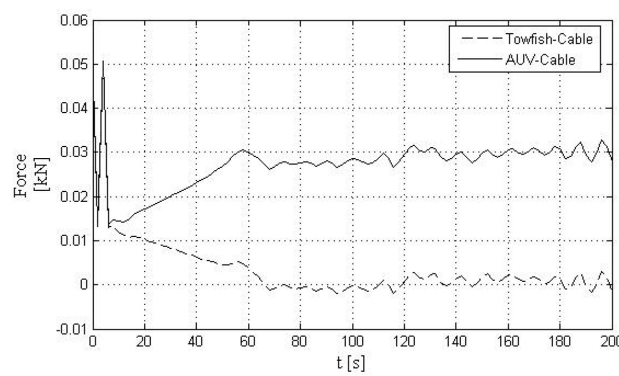

Fig. 19 Effective Tension during Vertical Zig Zag Maneuver.

IV. DISCUSSION

The simulation results have been used to meet the objectives of determining an appropriate cable length and thrust to be used in future field experiments. In addition, the effects of different current speeds have also been determined.

The first objective was to determine an appropriate cable length for various maneuvers. Shorter cable lengths allowed the towfish to survey a larger area while being towed behind the AUV during circle maneuvering. As the cable length increased to 15 m, the towfish trajectory was off from the AUV trajectory by at least 3 m throughout the entire circle maneuver.

The average depth of the towfish was also significantly dependent on the cable length even though the depth of the AUV remained constant at 30 m. During the circle maneuver, the 5 m cable length was short enough to keep the towfish between 29 m to 32.5 m depth, which was almost equivalent to the AUV depth. The 9 m cable caused the towfish to travel between the 32 to 35 m depth range, and the 15 m cable caused it to travel between 39 m to 42 m depth. Similar results were shown for the vertical zig zag maneuvers. The towfish covered approximately 5 m of vertical distance for each cable length, but at different depths that were approximately equal to the depths experienced with the circle maneuver. Therefore, the AUV depth will need to be decreased as the cable length is increased so that the towfish will travel at the appropriate depth of interest for both circle and zig zag maneuvering until the cable gets so long that it reaches critical tow angle.

The second objective was to determine an appropriate tow speed or AUV percent thrust for each maneuver. During vertical zig zag maneuvering, x position of the towfish increased by approximately 20 m from the change of 40% to 80% thrust. The y position only changed about 0.2 m and z position remained the same. When the angle of sternplane oscillations was increased from 5 degrees to 15 degrees, similar results were shown, which proves the percent thrust to have the same effect on the maneuver regardless of the angle of sternplane deflection. During circle maneuvering, the towfish traveled a further distance with larger percent thrust and covered a larger area as expected.

Changes in percent thrust had a more significant impact on the pitch angle of the towfish during circle maneuvering. For all of the thrust values tested, the towfish stayed below the 90 degree pitch sensory dead zone during circle maneuvers. However, at slower speeds, such as 40% thrust, the pitch angle approached 80 degrees. When the AUV traveled at 80% thrust, the pitch angle of the towfish did not exceed 50 degrees. After decreasing the distance between the center of gravity and the center of buoyancy from 0.0118 m to 0.0018 m, the same 40% and 80% thrust circle maneuvers showed great improvement on pitch angles. The 40% thrust pitch angle reduced to 30 degrees, and the 80% thrust pitch angle reduced to 10 degrees. This lower pitch angle is much more favorable for stability and to ensure the towfish does not come close to the dead zone angle of the sensor.

Changes in current speed had a significant effect on the towfish trajectory during circle maneuvering. The trajectory plots appeared to take on a spiral shape as expected. For each case the surface current was increased 0.75 m/s, and both the AUV and towfish trajectory looked less like a spiral and more like a zig zag. At a surface current speed of 1.25 m/s, both bodies moved completely in a zig zag formation during circle maneuvers. Towfish trajectory during zig zag maneuvers was not significantly affected when the current was increased.

Effective tension at both the towfish-cable and AUV-cable connection was much greater during circle maneuvering than vertical zig zag maneuvering. Tension reached a maximum of 0.12 kN and 0.05 kN during circle and zig zag maneuvering, respectively.

V. Conclusions

The Bluefin AUV and Seaspy magnetometer towfish will be used in future experiments to determine the magnetic fluctuations caused by internal waves. The results indicate that a 5 m tow cable provides the best maneuverability of the towfish in comparison to the longer cables. The towfish traveled greater distance in a given period of time and more closely followed the waypoints of the AUV in not only the x and y directions, but in the vertical direction as well. The longer tow cables gave the towfish too much freedom to stray off course during maneuvering of the AUV.

Tow speeds between 60% and 80% thrust provided better orientation angles than the slower tow speeds. However, the cause for the high pitch angles was determined to be the distance between the center of gravity and center of buoyancy. Once this distance was decreased, the pitch angle decreased significantly. While 80% thrust showed the best orientation results, this fast speed may not be desirable when attempting to collect magnetic field data on the towfish. A tow speed between 60% and 70% would be more appropriate for the planned field experiments.

Surface current speeds between 0.25 m/s and 1.25 m/s altered the courses of the AUV and towfish during circular maneuvering. As the surface current speed increased up to 1.25 m/s, the spiral course changed to a zig zag course for both the AUV and towfish.

Acknowledgment

Special thanks to Dr. W. Venezia, Prof. P. E. An and Mr. Eric Dykes for their technical input on the simulations.

References

[1] Allen, G. I., Matthews, R., & Wynn, M. (2001) "Mitigation of Platform Generated Magnetic Noise Impressed on a Magnetic Sensor Mounted in an Autonomous Underwater Vehicle". MTS/IEEE OCEANS 2001, (pp. 63-71). Honolulu.

[2] Allen, G., Sulzberger, G., Bono, J., Pray, J., & Clem, T. (2005) "Initial evaluation of the new real-time tracking gradiometer designed for small unmanned underwater vehicles". MTS/IEEE OCEANS 2005, (pp. 1956-1962). Washington.

[3] Allmendinger, E. (1990) Submersible Vehicle Systems Design. Society of Naval Architects and Marine Engineers, Jersey City, NJ.

[4] Avera, W., Gallacher, P. C., Teague, W., Liang, R., & Nelson, J. B. (2009) "Magnetic Noise Associated with Ocean Internal Waves". MTS/IEEE OCEANS 2009 - Marine Technology for Our Future: Global and Local Challenges, (pp. 1-4). Biloxi.

[5] Bluefin Robotics Corporation. (2004) FAU: AUV Specfication and Procedures. Bluefin Robotics, Cambridge, MA.

[6] Bono, J., Overway, D., & Wynn, W. (2003) "Magnetic Sensor Operation Onboard a UUV: Magnetic Noise Investigation using a Total-Field Gradiometer". MTS/IEEE OCEANS 2003, (pp. 2018-2022).

[7] Carlton, J. (2007) Marine Propellers and Propulsion. Elsevier, Burlington, MA.

[8] Clabon, M. (2003) Thermocline Tracking Using an Upgraded Ocean Explorer Autonomous Underwater Vehicle. M.S. Thesis Department of Ocean Engineering, Florida Atlantic University, Dania Beach, FL 33004.

[9] Dhanak, M. An, P. E. and Holappa, K. An (2001) AUV Survey in the littoral zone: small-scale subsurface variability accompanying synoptic observations of surface currents. IEEE J. Oceanic Engng. 26(4):752-768.

[10] Greenwood, D. (1988) Principles of Dynamics. Prentice-Hall, Englewood Cliffs, NJ.

[11] Hrvoic, D. (2007) SeaSPY Overhauser Magnetometer Technical Applications Guide. Marine Magnetics, Corp.

[12] Leonard, N. (1997) Stability of a Bottom-heavy Underwater Vehicle. Automatica, 331-346.

[13] Miller, L. (2011) Simulating the Dynamic Interaction of an AUV and Towed Magnetometer. M.S. Thesis, Department of Ocean & Mechanical Engineering, Florida Atlantic University, Boca Raton, FL.

[14] Rentschler, M. E. (2003) Dynamic Simulation Modeling and Control of the Odyssey III Autonomous Underwater Vehicle. M.S. Thesis, Department of Mechanical Engineering, Massachusetts Institute of Technology, Cambridge, MA.

[15] Rentschler, M., Hover, F., & Chryssostomidis, C. (2006) System Identification of Open-Loop Maneuvers Leads to Improved AUV Flight Performance. IEEE J. Oceanic Engng. 31(1): 200-208.

[16] Schuch, E. M. (2004) Towfish Design, Simulation and Control. M.S. Thesis, Virginia Polytechnic Institute and State University, Blacksburg, VA.

[17] Schuch, E., Linklater, A., Lambeth, N., & Woolsey, C. (2005) "Design and Simulation of a Two Stage Towing System". MTS/IEEE OCEANS 2005, (pp. 1705-1712). Washington, DC.

[18] Teixeira, F., Aguiar, A., & Pascoal, A. (2006) Nonlinear Control of an Underwater Towed Vehicle. 7th IFAC Conference on Maneuvering and Control of Marine Craft. Lisbon, Portugal.

[19] Wynn, M., & Bono, J. (2002). "Magnetic sensor operation onboard an AUV: magnetic noise issues and a linear systems approach to mitigation". MTS/IEEE OCEANS 2002, (pp. 985-993).